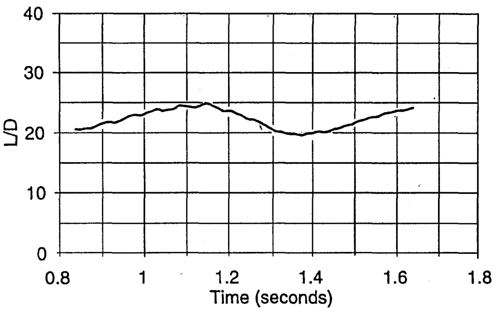

a) Six-percent camber rigid wing

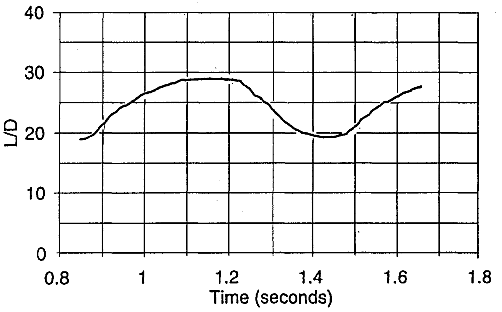

b) Latex membrane wing, which exhibits about 6% camber at 35.4 fps

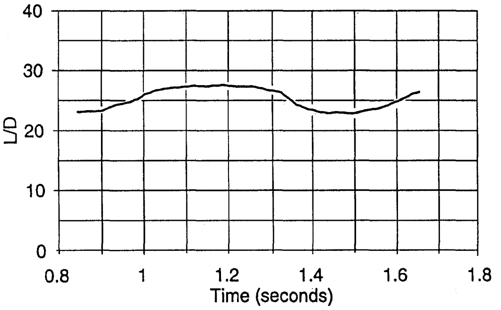

c) Hybrid wing with curved wire screen camber stop

Fig. 5 Experimental time series at $Re = 7.5 \times 10^4$, $Sr = 0.10$, and angle of attack = 7 deg.

approximate 6% camber at this mean velocity, and so the results can be reasonably compared with the simulation flexible airfoil with an initial camber value. Because many hundreds of cycles take place before the data are recorded, this is a limiting cycle case, unlike the case examined in the numerical simulations.

Figure 5 shows measured lift-to-drag ratios throughout one complete cycle for the three test airfoils described. The 6% camber rigid wing (shown in Fig. 5a) exhibits a mild sensitivity to the velocity variation. The membrane covered flat wing, which was observed to fluctuate around approximately 6% camber, is shown in Fig. 5b. Substantial variation in the lift-to-drag ratio is observed, consistent with what would be expected with the observed changes in camber as the velocity changes. The lift-to-drag ratio is improved during the accelerating part of the cycle; however, some degradation in performance occurs during the decelerating portion. Finally, the hybrid wing with the curved screen insert gives the results shown in Fig. 5c. The sensitivity to velocity variation is smaller than that of the pure flexible wing, and yet the overall performance is higher.

Conclusions

The focus of the present study is on the aerodynamic performance of the μAV in low Reynolds number unsteady flows. Each of the experimental wings showed behavior qualitatively similar to that shown in their numerical simulation counterparts, even though the shapes and construction features were not exactly the same, as mentioned. The hybrid wing in particular demonstrated that it is possible to combine improvements during accelerating flows with sustained performance during deceleration. It seems likely that, by using more aggressive and more active adaptation strategies than the very simple ones presented here, practical μAV wings with improved performance qualities can be realized.

Acknowledgments

The present effort has been sponsored in part by a grant from The Boeing Company. We are grateful for the contributions of Richard Fearn and Thomas Marin in the experimental setup.

References

[1]Smith, R. W., and Shyy, W., "Computation of Unsteady Laminar Flow over a Flexible Two-Dimensional Membrane Wing," *Physics of Fluids*, Vol. 7, No. 8, 1995, pp. 2175–2184.

[2]Smith, R., and Shyy, W., "Computational Model of Flexible Membrane Wings in Steady Laminar Flow," *AIAA Journal*, Vol. 33, No. 10, 1995, pp. 1769–1777.

[3]Shyy, W., Udaykumar, H. S., Rao, M. M., and Smith, R. W., *Computational Fluid Dynamics with Moving Boundaries*, Taylor and Francis, Washington, DC, 1996, Chap. 3.

[4]Menter, F. R., "Two-Equation Eddy-Viscosity Turbulence Models for Engineering Applications," *AIAA Journal*, Vol. 32, No. 8, 1994, pp. 1598–1605.

[5]Shyy, W., *Computational Modeling for Fluid Flow and Interfacial Transport*, Elsevier, Amsterdam, 1994, Chap. 5.

[6]Smith, R. W., and Shyy, W., "Computation of Aerodynamic Coefficients for a Flexible Membrane Airfoil in Turbulent Flow: A Comparison with Classical Theory," *Physics of Fluids*, Vol. 8, No. 12, 1996, pp. 3346–3353.

[7]Shyy, W., and Smith, R. W., "A Study of Flexible Airfoil Aerodynamics with Application to Micro Aerial Vehicles," AIAA Paper 97-1933, June 1997.

[8]Al-Asmi, K., and Castro, I. P., "Production of Oscillatory Flow in Wind Tunnels," *Experiments in Fluids*, Vol. 15, Jan. 1993, pp. 33–41.

A. Plotkin
Associate Editor

Improvements to a Dual-Time-Stepping Method for Computing Unsteady Flows

S. DeRango* and D. W. Zingg†
University of Toronto,
Downsview, Ontario M3H 5T6, Canada

Introduction

IMPLICIT time-marching methods are preferred for computing many unsteady aerodynamic flows because of physical and numerical stiffness. However, a fully implicit method can be expensive because the solution of a nonlinear problem is required at each time step. The approximately factored algorithm of Beam and Warming with local time linearization[1] is an efficient option, capable of retaining both second-order accuracy in time and unconditional stability. In practice, first-order time accuracy is often obtained as a result of approximate linearization of the artificial dissipation and turbulence models, low-order treatment of boundary and interface conditions, and loose coupling of a field-equation turbulence model. An alternative approach, which has become popular in recent years, is to apply an algorithm developed for steady flows to the nonlinear problem arising at each iteration of the implicit time-marching method.[2–8] Thus one can apply an algorithm with non-time-accurate convergence acceleration techniques such as local preconditioning, local time stepping, diagonalization, and multigrid. Such methods are typically called dual-time-stepping or subiteration methods.

Received June 12, 1996; presented as Paper 96-2088 at the AIAA 2nd Fluid Dynamics Conference, New Orleans, LA, June 17–20, 1996; revision received April 21, 1997; accepted for publication April 30, 1997.

*Graduate Student, Institute for Aerospace Studies, 4925 Dufferin Street.

†Associate Professor, Institute for Aerospace Studies, 4925 Dufferin Street. Member AIAA.

The nonlinear problem to be solved within an implicit time-marching method has several differences from a typical steady-state problem. The initial guess is usually quite good, and the degree of convergence required is quite small, perhaps a few orders of magnitude reduction in residual. Therefore, algorithms developed for steady problems may not be optimal for use in a dual-time context. In this Note, we present some modifications to the diagonal approximately factored algorithm that lead to savings in a dual-time-stepping context.

Governing Equations and Numerical Method

The governing equations are the two-dimensional thin-layer Navier–Stokes equations, written in generalized coordinates as

$$\partial_t \hat{Q} + \partial_\xi \hat{E} + \partial_\eta \hat{F} = Re^{-1}\partial_\eta \hat{S} \tag{1}$$

where $\hat{Q}$ contains the conservative flow variables and $\hat{E}$ and $\hat{F}$ are the flux vectors in the ξ and η directions, respectively. $\hat{S}$ contains the viscous terms. Second-order central spatial differences are used with second- and fourth-difference nonlinear artificial dissipation, as in ARC2D.[9]

Applying the second-order backward method to the discretized form of Eq. (1), one obtains

$$G(\hat{Q}^{n+1}) \equiv \frac{3\hat{Q}^{n+1} - 4\hat{Q}^n + \hat{Q}^{n-1}}{2\Delta t} + \left[\delta_\xi \hat{E}(\hat{Q}^{n+1}) + \delta_\eta \hat{F}(\hat{Q}^{n+1}) - Re^{-1}\delta_\eta \hat{S}(\hat{Q}^{n+1})\right] = 0 \tag{2}$$

where $\hat{Q}^n = \hat{Q}(n\Delta t)$ and δ denotes a generic spatial operator. This is the nonlinear relation we wish to satisfy at each time step. Linearization and approximate factorization lead to the following form, which is second-order accurate in time:

$$\left[I + \tfrac{2}{3}\Delta t\delta_\xi \hat{A}^n\right]\left[I + \tfrac{2}{3}\Delta t\delta_\eta \hat{B}^n - \tfrac{2}{3}\Delta t \mathcal{R}e^{-1}\delta_\eta \hat{M}^n\right]\Delta\hat{Q}^n = \hat{R}^n \tag{3}$$

where

$$\hat{R}^n = -\tfrac{2}{3}\Delta t\left[\delta_\xi \hat{E}(\hat{Q}^n) + \delta_\eta \hat{F}(\hat{Q}^n) - \mathcal{R}e^{-1}\delta_\eta \hat{S}(\hat{Q}^n)\right] + \tfrac{1}{3}\Delta\hat{Q}^{n-1} \tag{4}$$

The matrices $\hat{A}$, $\hat{B}$, and $\hat{M}$ are the flux Jacobians. With fourth-difference implicit artificial dissipation, the solution of a block pentadiagonal system of equations is required. This scheme is referred to as the BPD scheme from this point onward.

For steady computations, the diagonal form of Eq. (3) can be used. It is given by

$$T_\xi[I + \alpha\delta_\xi \Lambda_\xi]\hat{N}[I + \alpha\delta_\eta \Lambda_\eta]T_\eta^{-1}\Delta\hat{Q}^n = \hat{R}^n \tag{5}$$

where $\hat{N} = T_\xi^{-1}T_\eta$. The matrices Λ_ξ and Λ_η are diagonal matrices whose elements are the eigenvalues of the flux Jacobians, including a contribution from the viscous flux Jacobian.[9] The matrix T_ξ has the eigenvectors of $\hat{A}$ as columns, and T_η has the eigenvectors of $\hat{B}$ as columns. The diagonal algorithm requires the solution of a scalar pentadiagonal system of equations and has proven to be three to four times faster than the BPD scheme. Unfortunately, it is first-order accurate in time and nonconservative, thus making it unsuitable for unsteady transonic flows. However, the diagonal form is ideally suited for use in a subiteration method.

Dual-Time-Step Subiteration Scheme

A "pseudo" time derivative is introduced to solve the nonlinear problem given by Eq. (2), as follows:

$$\frac{\partial \hat{Q}}{\partial \tau} = -G(\hat{Q}) \tag{6}$$

Many different methods can be used to solve Eq. (6). We use the diagonal form of the approximately factored algorithm. Applying implicit Euler time marching to Eq. (6) gives

$$\frac{\hat{Q}^{p+1} - \hat{Q}^p}{\Delta\tau} = -\frac{3\hat{Q}^{p+1} - 4\hat{Q}^n + \hat{Q}^{n-1}}{2\Delta t} - \left(\delta_\xi \hat{E}^{p+1} + \delta_\eta \hat{F}^{p+1} - Re^{-1}\delta_\eta \hat{S}^{p+1}\right) \tag{7}$$

where $\Delta\tau$ is the pseudo-time-step size. Thus the dual-time-stepping scheme, in diagonal form, may be written as follows:

$$T_\xi[\Gamma + \Delta\tau\delta_\xi \Lambda_\xi]\hat{N}_d[\Gamma + \Delta\tau\delta_\eta \Lambda_\eta]T_\eta^{-1}\Delta\hat{Q}^p = -\Delta\tau G(\hat{Q}^p) \tag{8}$$

where $\Gamma = [(3/2\Delta t) + (3\Delta\tau/2\Delta t)]I$ and $\hat{N}_d = T_\xi^{-1}\Gamma^{-1}T_\eta$.

The algebraic Baldwin–Lomax[10] and one-equation Spalart–Allmaras[11] turbulence models are described in detail in the given references. Both models are decoupled from the Navier–Stokes equations. In the Spalart–Allmaras model, the partial-differential equation is solved using the second-order backward time-marching method with an approximately factored dual-time-stepping scheme, similar to the mean-flow equations.

Modified Subiteration Method

We now introduce two further approximations to the implicit operator used for the subiterations: 1) second-difference dissipation is used in the implicit operator, leading to a scalar tridiagonal form and 2) the Jacobian matrices are frozen during the subiterations.

The dissipation scheme on the left-hand or implicit side of Eq. (8) is modified to reduce the matrix to a scalar tridiagonal form. The original nonlinear dissipation scheme is still used on the right-hand side. The second-difference coefficients on the implicit side are replaced by a value equal to the second-difference coefficients on the explicit side plus the fourth-difference coefficients multiplied by some factor ε. A value of ε equal to 2 or 3 works well. This scheme will be referred to as the tridiagonal subiteration scheme.

Solution of the banded system constitutes a significant portion of the computational effort in solving for $\Delta\hat{Q}^p$. To avoid repetitive solution of a system that does not change very much during the subiteration process, the eigenvalues of the flux Jacobians are frozen during the subiterations at each time step. An LU decomposition is used to decompose and store $[\Gamma + \Delta\tau\delta_\xi \Lambda_\xi]$ in Eq. (8) after the first iteration at each time step. The same is done for the η sweep. The eigenvector matrices denoted by T_ξ and T_η, however, are not frozen.

Results

Laminar flow over the NACA 0012 airfoil was computed at a Mach number of 0.2, a Reynolds number of 800, and an angle of attack of 20 deg. A coarse C mesh (169 × 49) was used because we were concerned here with time accuracy only. Figure 1 shows the reduced frequency of shedding $\kappa = nc/u_\infty$ as a function of computational effort, where n is the frequency and c is the chord length. One work unit is equivalent to 200 sweeps of the diagonal algorithm. The points shown were computed with different values of Δt. As Δt decreases, the computational effort increases. Three subiterations are used at each time step. All of the methods shown converge to the same reduced frequency as Δt is decreased. The basic dual-time-stepping method is much more efficient than the BPD scheme. Compared to the basic subiteration scheme, the tridiagonal subiteration

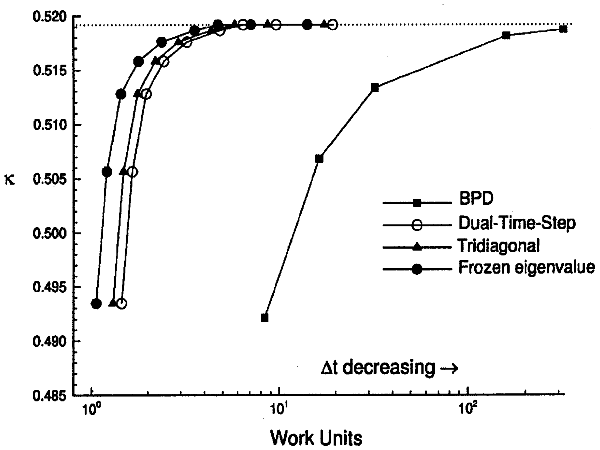

Fig. 1 Reduced frequency vs CPU work per period using various schemes for NACA 0012 airfoil (Mach number = 0.2, $Re = 800$, and $\alpha = 20$ deg).

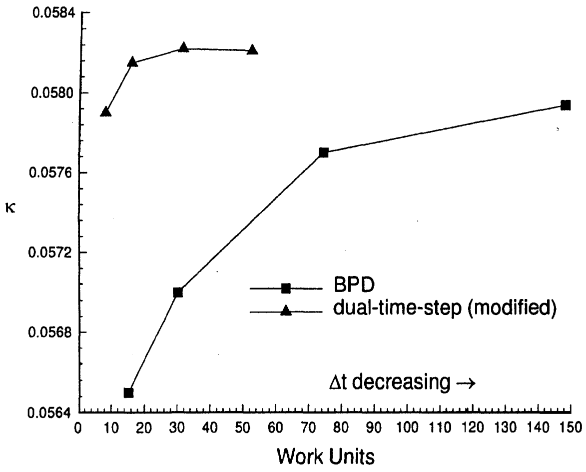

Fig. 2 Reduced frequency vs CPU work per period using the modified dual-time-stepping and BPD schemes with Baldwin–Lomax turbulence model for NACA 0012 airfoil (Mach number = 0.7, $Re = 9 \times 10^6$, and $\alpha = 6$ deg).

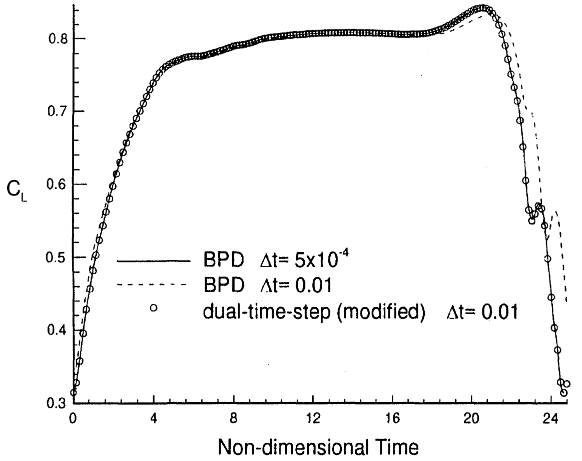

Fig. 3 Coefficient of lift vs nondimensional time using the modified subiteration and BPD schemes with Baldwin–Lomax turbulence model for NACA 0012 airfoil (Mach number = 0.7, $Re = 9 \times 10^6$, and $\alpha = 6$ deg).

scheme reduces the CPU expense approximately 10%, whereas the frozen eigenvalue scheme produces CPU savings of up to 30%.

Turbulent flow over a NACA 0012 airfoil was computed at a Mach number of 0.7, a Reynolds number of 9×10^6, and an angle of attack of 6 deg. Under these conditions, the airfoil experiences self-induced periodic shock oscillations. This case was run on a 331 × 51 C mesh.

Baldwin–Lomax Model

With this model, we used four subiterations. This generally produced a final residual [in Eq. (8)] of about 10^{-10}. Figure 2 compares the modified dual-time-stepping method, including both the frozen eigenvalue and the tridiagonal operator, with the BPD method. One work unit is equivalent to 1000 sweeps of the diagonal algorithm. The modified method requires approximately 35% less CPU time than the basic method. To obtain a reduced frequency within 0.5% of the converged value, the modified dual-time-stepping method requires roughly $\frac{1}{20}$ of the CPU time of the BPD scheme. Figure 3 shows that the dual-time-stepping approach produces equivalent accuracy to the BPD scheme at much higher values of Δt.

Spalart–Allmaras Model

Three mean-flow subiterations were used with the Spalart–Allmaras model. After each mean-flow subiteration, turbulence-model subiterations were performed until the turbulence-model residual was reduced by two orders of magnitude. This typically required 30–60 turbulence-model subiterations. Figure 4 compares the modified dual-time-stepping scheme with the BPD scheme. For this case, each work unit represents 1000 minutes on a Silicon Graphics R4000 workstation. The dual-time-stepping method produces a

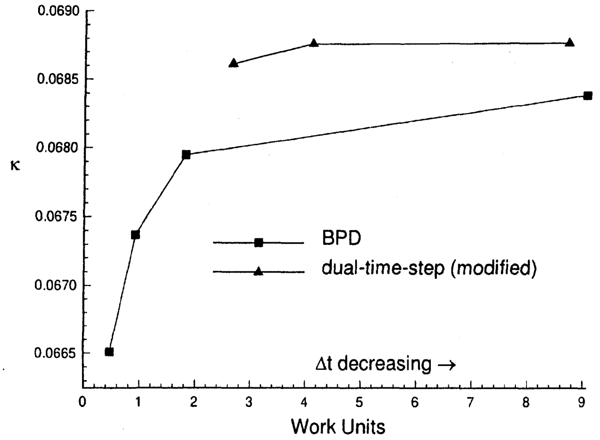

Fig. 4 Reduced frequency vs CPU work per period using the modified dual-time-stepping and BPD schemes with Spalart–Allmaras turbulence model for NACA 0012 airfoil (Mach number = 0.7, $Re = 9 \times 10^6$, and $\alpha = 6$ deg).

converged value of the reduced frequency with fewer than four work units, whereas the BPD scheme is still quite far from the converged value with a Δt of 5×10^{-4}, requiring nine work units.

Conclusions

Dual-time-stepping implementations of implicit time-marching methods are an efficient option for computing unsteady flows. The associated subiterations can reduce linearization and factorization errors resulting from some methods, and, more importantly, they can reduce first-order errors resulting from boundary and interface conditions, approximate linearizations, and loosely coupled turbulence models. We have presented two easy-to-implement modifications to a dual-time-stepping scheme using the diagonal form of an approximate factorization algorithm that produce CPU savings of about 35%.

Acknowledgments

Funding from de Havilland, Inc., and the Natural Science and Engineering Research Council of Canada is gratefully acknowledged.

References

[1]Beam, R. M., and Warming, R. F., "An Implicit Factored Scheme for the Compressible Navier–Stokes Equations," *AIAA Journal*, Vol. 26, No. 4, 1978, pp. 393–402.

[2]Chakravarthy, S. R., and Osher, S., "Numerical Experiments with the Osher Upwind Scheme for the Euler Equations," *AIAA Journal*, Vol. 21, No. 9, 1983, pp. 1241–1248.

[3]Rai, M. M., and Chakravarthy, S. R., "An Implicit Form for the Osher Upwind Scheme," *AIAA Journal*, Vol. 24, No. 5, 1986, pp. 735–743.

[4]Alonso, J., Martinelli, L., and Jameson, A., "Multigrid Unsteady Navier–Stokes Calculations with Aeroelastic Applications," AIAA Paper 95-0048, Jan. 1995.

[5]Arnone, A., Liou, M.-S., and Povinelli, L. A., "Integration of Navier–Stokes Equations Using Dual Time Stepping and a Multigrid Method," *AIAA Journal*, Vol. 33, No. 6, 1995, pp. 985–990.

[6]Venkateswaran, S., and Merkle, C. L., "Dual Time Stepping and Preconditioning for Unsteady Computations," AIAA Paper 95-0078, Jan. 1995.

[7]Rumsey, C. L., Sanetrik, M. D., Biedron, R. T., Melson, N. D., and Parlette, E. B., "Efficiency and Accuracy of Time-Accurate Turbulent Navier–Stokes Computations," AIAA Paper 95-1835, July 1995.

[8]Pulliam, T. H., "Time Accuracy and the Use of Implicit Methods," AIAA Paper 93-3360, July 1993.

[9]Pulliam, T. H., "Efficient Solution Methods for the Navier–Stokes Equations," Lecture Notes for von Kármán Inst. for Fluid Dynamics Lecture Series: Numerical Techniques For Viscous Flow Computation In Turbomachinery Bladings, von Kármán Inst., Brussels, Belgium, Jan. 1986.

[10]Baldwin, B., and Lomax, H., "Thin-Layer Approximation and Algebraic Model for Separated Turbulent Flows," AIAA Paper 78-257, Jan. 1978.

[11]Spalart, P. R., and Allmaras, S. R., "A One-Equation Turbulence Model for Aerodynamic Flows," AIAA Paper 92-0439, Jan. 1992.

J. Kallinderis
Associate Editor